

# Quantitative imaging of tumour glucose uptake using glucoseCEST: comparison with <sup>18</sup>F-FDG autoradiography

Simon Walker-Samuel<sup>1</sup>, Rajiv Ramaswamy<sup>1</sup>, Francisco Torrealdea<sup>2</sup>, Marilena Rega<sup>2</sup>, Peter Johnson<sup>3</sup>, Vineeth Rajkumar<sup>3</sup>, Simon Richardson<sup>1</sup>, Dave Thomas<sup>2</sup>, Barbara Pedley<sup>3</sup>, Mark F. Lythgoe<sup>1</sup>, and Xavier Golay<sup>2</sup>

<sup>1</sup>Centre for Advanced Biomedical Imaging, University College London, London, United Kingdom, <sup>2</sup>Institute of Neurology, University College London, United Kingdom, <sup>3</sup>Cancer Institute, University College London, United Kingdom

\* MFL and XG are joint senior authors

**Introduction.** Tumours display a greater reliance on aerobic glycolysis than normal tissues, a phenomenon known as the Warburg effect. This is a key discriminator of tumours from normal tissues, which has highlighted it as a target for anticancer therapy [1] and as a marker for the identification and characterization of malignant disease. The ability to non-invasively probe tumour glucose uptake and usage is of key importance, in particular as raised glucose uptake is indicative of greater malignancy [2] and can potentially be used as a marker of response to therapy. We have recently developed a technique for evaluating the uptake of glucose in tumours named glucoseCEST, which utilises the exchange of labelled protons between hydroxyl groups and bulk tissue water [3,4]. Here we describe a method for quantifying absolute glucose concentration from glucoseCEST data, evaluate it in two colorectal tumour xenograft models (SW1222 and LS174T), and compare it with <sup>18</sup>F-FDG autoradiography.

**Theory.** GlucoseCEST utilises the exchange of pre-saturated protons in glucose hydroxyl groups and bulk water to reduce the measured signal from water. The measured asymmetric magnetisation transfer ratio can be described analytically by Eq. 1 (left) [5], where  $x_{gl} = 5[gl]/2[H_2O]$  is the fraction of exchangeable glucose (gl) protons,  $k$  is the OH proton exchange rate,  $R_{1w}$  is the longitudinal relaxation rate of water,  $\alpha$  is the saturation factor (assumed to be 1) and  $t_{sat}$  is the saturation time. Thus, the change in the area under the  $MTR_{asym}$  curve following glucose injection (named here the glucoseCEST enhancement (GCE)), in the absence of any other changes, is proportional to glucose concentration. In this study, phantom data are used to provide an empirical calibration for *in vivo* measurements of glucose concentration. As the proton exchange rate is pH-dependent, measurements of pH from <sup>31</sup>P MRS data were carried out to identify the appropriate set of calibration factors (see Fig. 1).

**Methods and Materials.** *Phantom experiments:* Ten solutions of glucose were prepared at concentrations ranging from 1 to 500 mM. Each solution was prepared four times, each with a different pH (6.4, 6.8, 7.2 or 7.6), by addition of hydrochloric acid or potassium hydroxide. During MRI scanning on a 9.4T Agilent VNMRS system and 39mm volume coil, the temperature of the phantoms was maintained at 37°C. GlucoseCEST data were acquired using a gradient echo imaging sequence (TR=6.1ms, TE=2ms, flip=5°, FOV=30×30mm<sup>2</sup>, slice thickness 1mm, matrix size=128×128)

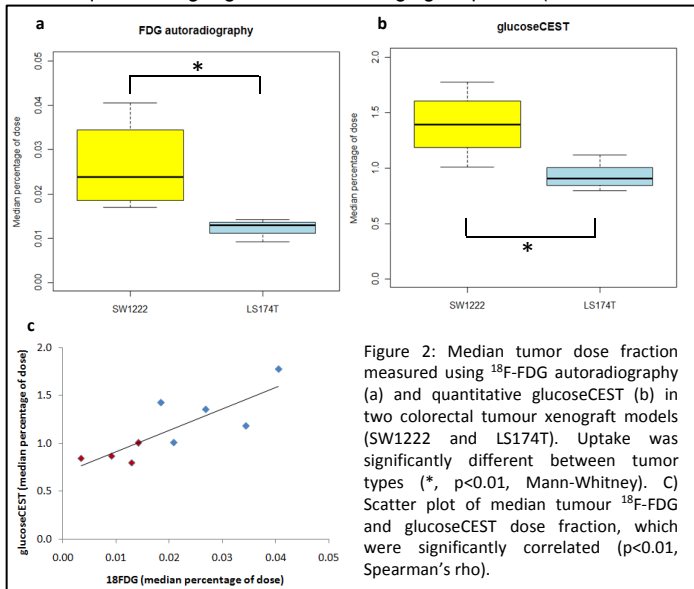


Figure 2: Median tumor dose fraction measured using <sup>18</sup>F-FDG autoradiography (a) and quantitative glucoseCEST (b) in two colorectal tumor xenograft models (SW1222 and LS174T). Uptake was significantly different between tumor types (\*,  $p<0.01$ , Mann-Whitney). C) Scatter plot of median tumor <sup>18</sup>F-FDG and glucoseCEST dose fraction, which were significantly correlated ( $p<0.01$ , Spearman's rho).

effects cause the relationship to plateau [5]. The gradients of these curves are dependent on pH, with greater enhancement characteristics with increasing pH. Using linear fits to these data and previous measurements of intracellular pH from <sup>31</sup>P MRS ( $7.2 \pm 0.1$  for SW122 and  $6.8 \pm 0.1$  for LS174T), GCE data from tumours were converted to glucose concentration. Both FDG autoradiography and glucoseCEST revealed significant differences between SW1222 and LS174T tumours ( $p<0.01$ , Mann-Whitney, see Figs. 2a and b). Furthermore, a significant correlation was observed between median glucose and FDG concentrations ( $p<0.01$ , Spearman's rho, see Fig. 2c). A strong correspondence can be seen between images of <sup>18</sup>F-FDG and glucose uptake (Fig. 3).

**Discussion:** We have presented an empirical method for quantifying glucose concentration from *in vivo* glucoseCEST measurements. We observed a significant difference between glucose uptake in SW1222 and LS174T tumours, which have previously been shown to display differing vascular and stromal phenotypes [6]. The same relationship was found in <sup>18</sup>F-FDG measurements, and glucose and <sup>18</sup>F-FDG uptake were significantly correlated. We have previously shown that no changes in blood flow or pH accompany the administration of glucose at the dose used in

this study [3]. Whilst the proposed technique is potentially sensitive to B1 inhomogeneity in calibration and/or *in vivo* data, and variations in tumour pH, this study provides proof of principle data and demonstrates its utility. It also suggests that glucoseCEST may provide corresponding information to FDG-PET, without the need to manufacture and administer a radiotracer.

**Acknowledgements:** King's College London and UCL Comprehensive Cancer Imaging Centre, CR-UK & EPSRC, in association with the MRC and DoH (England), British Heart Foundation. **References:** [1] Dang, et al., Journal of molecular medicine, 2011, 89, [2] Tanimoto, et al. Nuclear medicine communications, 2010, 31, [3] Walker-Samuel et al., Proc. ISMRM 2011, Montreal, #962, [4] Chan et al. Proc. ISMRM 2011, Montreal, #551, [5] van Zijl et al., PNAS, 2006, 104(11), [6] El Emir et al., Cancer Research, 2007, 67(24).

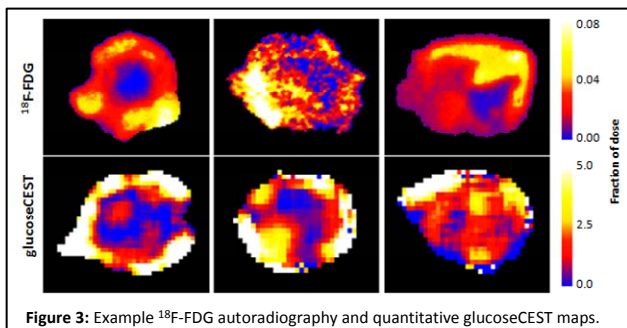


Figure 3: Example <sup>18</sup>F-FDG autoradiography and quantitative glucoseCEST maps.

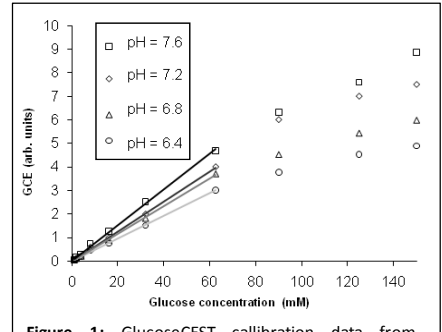


Figure 1: GlucoseCEST calibration data from phantoms, used to estimate glucose concentration *in vivo*.